Low degree gravity changes from GRACE, Earth rotation, geophysical models, and satellite laser ranging

J. L. Chen[1] and C. R. Wilson[1,2,3]

[1] Several independent time series of variations ΔC_{21}, ΔS_{21}, and ΔC_{20} in Earth's gravity field are compared for the period April 2002 to May 2007. We examine estimates from the Gravity Recovery and Climate Experiment (GRACE), Earth rotation variations, climate models, and satellite laser ranging (SLR). Recently released GRACE solutions show significant improvement relative to earlier results, especially for ΔC_{21} and ΔS_{21}. At the annual period, all estimates agree remarkably well, and good correlation is found among time series at intraseasonal periods. In general, Earth rotation values for ΔC_{21} and ΔS_{21}, and SLR values for ΔC_{20} agree best with GRACE estimates. GRACE ΔC_{20} time series are contaminated by aliased ocean tide model errors. SLR ΔC_{21} and ΔS_{21} time series have been reported without an ocean pole tide (OPT) correction and with an older Solid Earth Pole Tide (SEPT) model. After correcting for OPT and SEPT deficiencies, SLR ΔC_{21} and ΔS_{21} time series show improved agreement with other estimates.

1. Introduction

[2] Low degree spherical harmonic (SH) gravity changes are caused by large scale mass redistribution within the Earth system. Important sources include air and water movement within the atmosphere, oceans, hydrosphere, and cryosphere, and redistribution within the solid Earth due to tectonics and glacial isostatic adjustment. Air and water contributions dominate at periods less than a few years, providing global-scale measurement of climate processes (air, water, and ice mass redistribution) from geodetic observations. Satellite laser ranging (SLR) has been an effective technique for measuring low degree gravitational changes, with time series extending over more than two decades. SLR is especially useful in measuring the lowest degree even zonal harmonics (especially ΔC_{20}, also called -J2 in the literature), [e.g., *Yoder et al.*, 1983; *Rubincam*, 1984]. Most SLR satellites are at high altitudes, (e.g., ~5860 and 5620 km for LAGEOS I & II) making them less sensitive to changes at high SH degrees. On the other hand, their high altitude leads to a long life relative to lower altitude satellites, yielding long time series. [e.g., *Cheng and Tapley*, 2004]. A linear trend (~0.116 × 10⁻¹⁰ per year) in ΔC_{20} is well determined from SLR [e.g., *Yoder et al.*, 1983; *Rubincam*, 1984; *Cheng et al.*, 1997], and widely accepted as an effect of postglacial rebound (PGR) following the last glacial maximum [e.g., *Mitrovica and Peltier*, 1993; *Devoti*

et al., 2001]. Contemporary polar ice sheet melting also has a measurable impact on ΔC_{20} variations [e.g., *Dickey et al.*, 2002]. SLR also provides estimates of ΔC_{21} and ΔS_{21} but with less precision than ΔC_{20} [e.g., *Chen et al.*, 2000]. SLR estimates of ΔC_{21}, ΔS_{21}, and ΔC_{20} show variations over a broad frequency band, with seasonal variability most prominent [e.g., *Chao and Eanes*, 1995; *Dong et al.*, 1996; *Chen et al.*, 2000]. Advancements in processing methods, and tracking of multiple satellites have improved SLR estimates, especially of individual low degree zonal terms [*Cheng and Tapley*, 2004].

[3] Data-assimilating numerical models of Earth climate elements (atmosphere, oceans, and land hydrology) provide independent estimates of Earth's gravity changes. Models give time variations in global gridded fields of atmospheric surface pressure, ocean bottom pressure, and terrestrial water storage, that are generally consistent with geodetic observations [e.g., *Chao and Eanes*, 1995; *Dong et al.*, 1996; *Johnson et al.*, 1999]. Agreement has been very good between geophysical models and SLR measurements, especially for even zonal harmonics.

[4] Estimates of ΔC_{21}, ΔS_{21}, and ΔC_{20} may also be obtained from measured Earth Orientation Parameters (EOP), including polar motion (X, Y) and length-of-day (LOD). At periods less than a few years, EOP variations mainly arise from two sources: surface mass load variations (atmospheric surface pressure, ocean bottom pressure, and terrestrial water storage); and mass motion (winds and ocean currents). Excitation of X, Y, and LOD due to surface mass load variations are proportional to changes in SH degree-2 variations ΔC_{21}, ΔS_{21}, and ΔC_{20} [e.g., *Wahr*, 1982; *Eubanks*, 1993; *Gross et al.*, 2004a]. Thus estimates of ΔC_{21}, ΔS_{21}, and ΔC_{20} from measured Earth rotational changes are possible, provided that wind and ocean current

[1]Center for Space Research, University of Texas, Austin, Texas, USA.
[2]Department of Geological Sciences, University of Texas, Austin, Texas, USA.
[3]Jackson School of Geosciences, University of Texas at Austin, Austin, Texas, USA.

contributions can be estimated using numerical ocean and atmospheric models. Previous studies [e.g., *Chen et al.*, 2000; *Chen and Wilson*, 2003] indicate that this can be done, and that EOP estimates of ΔC_{21}, ΔS_{21}, and ΔC_{20} agree reasonably well with geophysical model predictions and SLR estimates.

[5] The Gravity Recovery and Climate Experiment (GRACE) is a twin satellite gravity mission jointly sponsored by the US National Aeronautics and Space Administration (NASA) and German Aerospace Center (DLR). Launched March 2002, GRACE measures Earth gravity with unprecedented accuracy by tracking changes in the distance between the two satellites and combining these measurements with data from on-board accelerometers and Global Positioning System (GPS) receivers. Now past its nominal 5-year life span, the GRACE mission is extended to beyond 2010 and promises continuous measurement of Earth gravity for 8 years or longer. GRACE provides Earth gravity as sets of SH coefficients at intervals of approximately 30 d [*Tapley et al.*, 2004]. Time variations in GRACE gravity fields have been shown to measure mass redistribution within the Earth system associated with a variety of climate processes [*Wahr et al.*, 1998, 2004].

[6] High SH degree and order coefficients in early GRACE fields such as release 1 (RL01) were contaminated by various artifacts, as were low degree coefficients, including ΔC_{21}, ΔS_{21}, and ΔC_{20} [*Chen et al.*, 2004]. A recently reprocessed GRACE data set, called release 4 (RL04), offers significantly improved data quality and spatial resolution, as demonstrated by recent studies [e.g., *Chen et al.*, 2007]. Although coefficients become progressively noisy at high degree and order, careful filtering leads to RL04 spatial resolution as fine as 300 km, at timescales exceeding one year, compared to 600 km or larger in RL01.

[7] Here we examine ΔC_{21}, ΔS_{21}, and ΔC_{20} variations for the period April 2002 to May 2007 provided by GRACE, EOP, climate models, and SLR. The objectives are: To evaluate RL04 GRACE estimates of ΔC_{21}, ΔS_{21}, and ΔC_{20}; Examine updated SLR multisatellite estimates; Reassess climate model performance at spatial and timescales observed by space geodesy; evaluate EOP estimates; and compare the four independent estimates of ΔC_{21}, ΔS_{21}, and ΔC_{20} at intraseasonal and seasonal timescales.

2. Data Processing

2.1. GRACE Estimates

[8] GRACE RL04 includes 58 approximately monthly average gravity solutions, from April 2002 to May 2007, from the Center for Space Research (CSR), University of Texas at Austin. RL04 SH coefficients are provided up to degree and order 60 [*Bettadpur*, 2007a]. RL04 is based upon a new background gravity model (a combination of GGM02C [*Tapley et al.*, 2005] and EGM96 [*Lemoine et al.*, 1998]); a new semidiurnal and diurnal ocean tide model (FES2004) [*Lyard et al.*, 2006]; and an updated solid Earth pole tide (SEPT) model following IERS2003 [*McCarthy and Petit*, 2003]. Ocean pole tide (OPT) effects are modeled using a self-consistent equilibrium model SCEQ from satellite altimeter data [*Desai*, 2002]. RL04 data processing standards are documented by *Bettadpur* [2007b]. Pole tide model additions and changes should improve GRACE estimates of ΔC_{21} and ΔS_{21} [*Chen et al.*, 2004].

[9] Nontidal atmospheric and oceanic contributions are removed from GRACE observations in the level-2 dealiasing process which employs data-assimilating numerical models of atmosphere and oceans. Each monthly field includes a separate file (GAC) with monthly average numerical model values of atmospheric and oceanic contributions removed in de-aliasing. To compare GRACE with EOP, SLR, and geophysical model estimates, GAC atmospheric and oceanic effects must be added to GRACE fields. A linear drift ($\sim 0.116 \times 10^{-10}$ per year) of ΔC_{20} (from SLR) is removed during GRACE data processing [*Bettadpur*, 2007b].

2.2. EOP Estimates

[10] Fully normalized ΔC_{21}, ΔS_{21}, and ΔC_{20} variations can be derived from EOP excitations after ocean current and wind effects are removed. These excitations (χ_i^{mass}, i = 1, 2, 3) are related to SH variations by [*Chen and Wilson*, 2003, equation (1)],

$$
\begin{aligned}
\Delta C_{21} &= -\left(1 + k_2'\right) \cdot \sqrt{\frac{3}{5}} \cdot \frac{(C-A)}{1.098 R^2 M} \cdot \chi_1^{mass} \\
\Delta S_{21} &= -\left(1 + k_2'\right) \cdot \sqrt{\frac{3}{5}} \cdot \frac{(C-A)}{1.098 R^2 M} \cdot \chi_2^{mass} \\
\Delta C_{20} &= -\left(1 + k_2'\right) \cdot \frac{3}{2\sqrt{5}} \cdot \frac{C_m}{0.753 R^2 M} \cdot \chi_3^{mass}
\end{aligned}
\tag{1}
$$

[11] Here M and R are mass and mean radius of the Earth, C and A (C-A = 2.61×10^{35} kg m^2) the two principal inertia moments of the Earth, and Cm (7.1236×10^{37} kg m^2) the principal inertia moment of Earth's mantle [*Eubanks*, 1993]. k_2' is the degree-2 load Love number (-0.301), accounting for elastic deformational effects on gravitational change. χ_i^{mass}(i = 1, 2, 3) can be computed from, $\chi_i^{mass} = \chi_i^{obs} - \chi_i^{motion}$ where, χ_i^{obs} are excitations from observed X, Y, and LOD time series, and χ_i^{motion} are wind and ocean current effects estimated from atmospheric and oceanic numerical models as described below.

[12] EOP time series are International Earth Rotation and Reference Systems (IERS) X, Y, and LOD series (05C04), which combine various space geodetic observations and are available from September 1962 to the present. Daily excitations from January 1962 to June 2007 were computed from the 05C04 series using the IERS online interactive tools (http://hpiers.obspm.fr/eop-pc/analysis/excitactive.html) with the Chandler period set at 433 d and the Chandler quality factor Q at 175. Tidal variations in LOD were removed. Decadal LOD variations, presumed to be related to core-mantle coupling, and a strong 5.6-year oscillation [*Chen et al.*, 2004] were removed via a low-cut filter with cutoff frequency set at 1 cycle in 4 years. After filtering, daily excitations from January 2002 to June 2007 were extracted for comparison with time series available from the other methods.

[13] Wind effects were computed from the National Centers for Environmental Prediction (NCEP) reanalysis (I) model [*Kalnay et al.*, 1996]. Wind fields include 17 pressure levels from 1000 mb to the model upper boundary at 10 mb. From equations given by *Eubanks* [1993], we computed daily time series from January 2002 to June 2007. As demonstrated by *Aoyama and Naito* [2000] and *Zhou et*
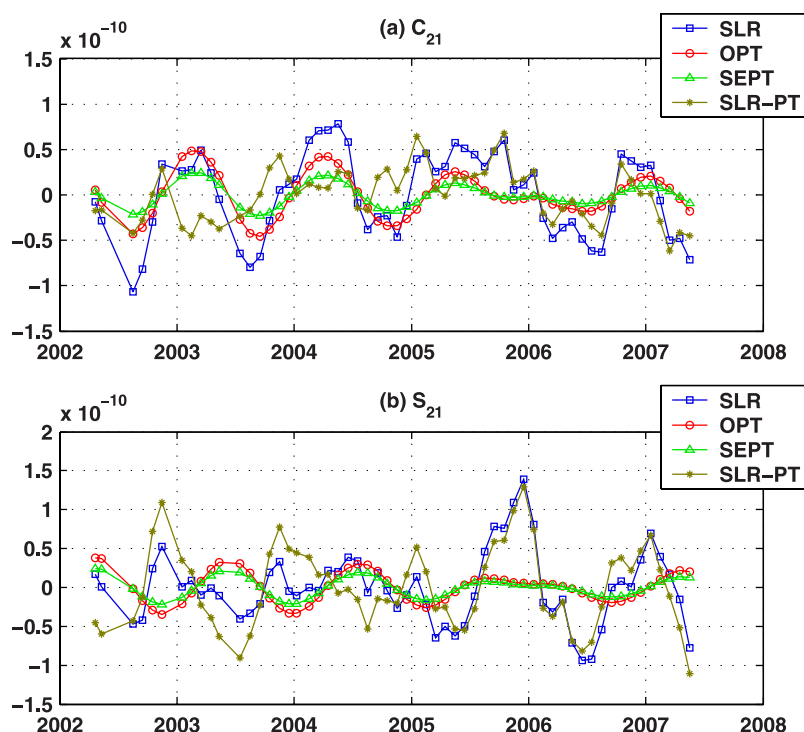
Figure 1. (a and b) SLR estimates of ΔC_{21} and ΔS_{21}, and pole tide (PT) contributions to ΔC_{21} and ΔS_{21}. OPT gives ocean pole tide contributions, SEPT accounts for solid pole tide effects due to the difference between earlier RL01 SEPT model and IERS2003 SEPT model in GRACE RL04. SLR-PT shows SLR estimates with both OPT and SEPT corrections applied.

al. [2006], atmospheric wind excitation estimates depend significantly on how topography is treated in the calculation. Here, we consider topographic effects by integrating wind momentum from the actual surface (not 1000 mb as commonly used) to the 10 mb level. This improves coherence between atmospheric excitation estimates and observations of EOP [*Zhou et al.*, 2006].

[14] Ocean current excitations were computed from (East, North) velocities (U,V) from the Estimating the Circulation and Climate of the Ocean (ECCO) data-assimilating ocean general circulation model (kf066b run) [*Fukumori et al.*, 2000]. (U,V) values are available at 10-day intervals, for 46 layers. Samples of ocean currents sampled every 10 d were interpolated to daily values before being subtracted from EOP series, along with wind effects. Then ΔC_{21}, ΔS_{21}, and ΔC_{20} variations from equation (1) were smoothed by a 30-day sliding window, and resampled in time to match the GRACE RL04 series.

2.3. Climate Model Predictions

[15] Data assimilating climate model estimates of ΔC_{21}, ΔS_{21}, and ΔC_{20} are the sum of GAC values from GRACE data files (representing ocean and atmosphere mass effects) and a land surface hydrological estimate from the global land data assimilation system (GLDAS) [*Rodell et al.*, 2004]. GLDAS uses a variety of data sources to compute water storage changes over most land areas, but omits the ice sheets of Greenland and Antarctica. Using equations (6)–(8) of *Wahr et al.* [1998], we computed hydrological contributions ΔC_{21}, ΔS_{21}, and ΔC_{20} from GLDAS 3-h values (including

soil moisture and snow water). The 3-h values were summed over each day to obtain a daily series and then smoothed with a 30-day moving average window. The smoothed series was then resampled to match GRACE (and GAC) sample times, and the sum of GAC and GLDAS estimates were then taken as the climate model prediction of gravity change. Thus GRACE and climate model time series have in common the GAC estimates of atmosphere and ocean mass redistribution.

2.4. SLR Estimates

[16] SLR estimates of monthly ΔC_{21}, ΔS_{21}, and ΔC_{20} variations from April 2002 to May 2007 are derived from laser tracking of multiple satellites, including Starlette, Ajisai, Stella, and LAGEOS 1 and 2 [*Cheng and Ries*, 2007]. These satellites are spherical, allowing surface forces to be modeled with great precision [*Cheng and Tapley*, 2004]. Models and other constants employed in SLR analysis follow GRACE RL01 standards [*Bettadpur*, 2003]. SLR estimates were provided by the GRACE project (courtesy of Minkang Cheng at CSR) in which they are used to validate GRACE estimates of degree-2 SH coefficients.

[17] A large contribution to ΔC_{21} and ΔS_{21} variations is from Earth rotational deformation due to polar motion, the pole tide (PT) [e.g., *Wahr*, 1985; *Chen et al.*, 2004]. The ocean pole tide (OPT) is not considered in the GRACE RL01 standards used in SLR calculations [*Bettadpur*, 2003]. Therefore we need to correct OPT effects in SLR estimates of ΔC_{21} and ΔS_{21}. RL01 standards also include a solid Earth pole tide (SEPT) model not consistent with IERS2003 Conventions [*McCarthy and Petit*, 2003]. Difference in the
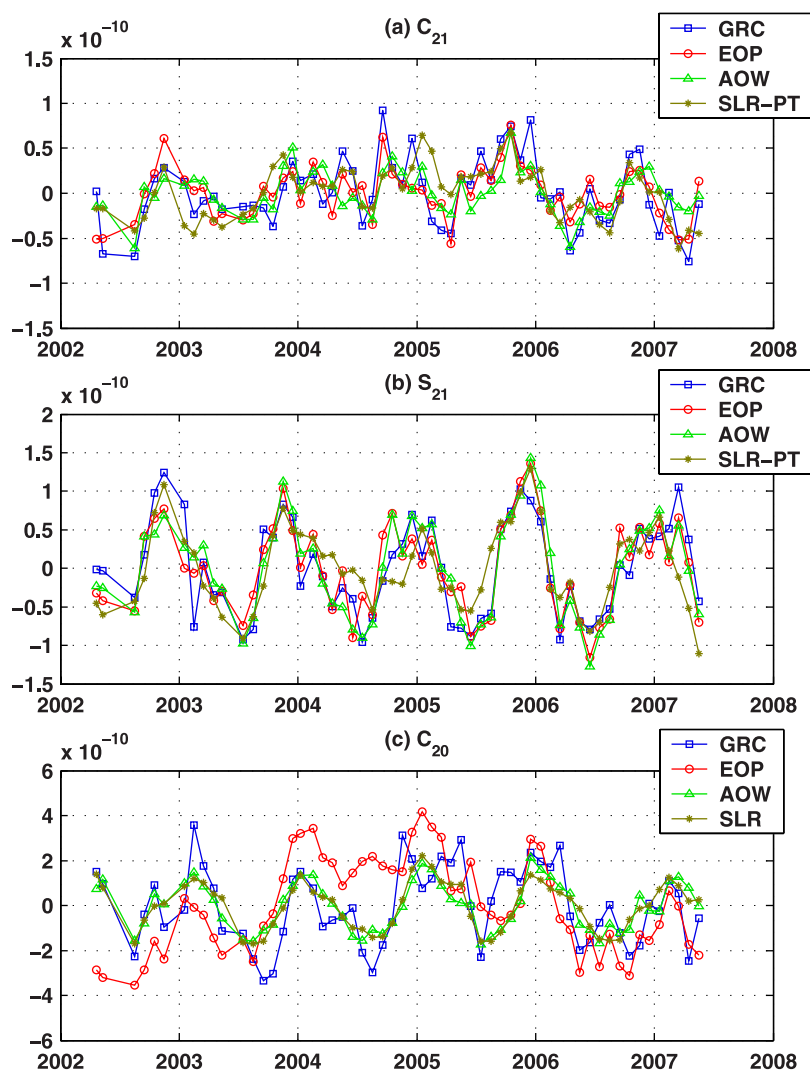
Figure 2. (a, b, and c) ΔC_{21}, ΔS_{21}, and ΔC_{20} estimates from GRACE (blue curves and squares), Earth rotation EOP (red curves and circles), and AOW models (green curves and triangles), and SLR (dark yellow curves and stars). All time series are averaged and resampled at GRACE time intervals.

SEPT convention may also affect comparisons between SLR and other estimates.

[18] We use the SCEQ OPT model [*Desai*, 2002] (as in GRACE RL04 standards) to calculate OPT effects on SLR ΔC_{21} and ΔS_{21}, with results shown in Figure 1. Figure 1 also shows possible effects of SEPT model differences between RL01 standards and IERS2003 Conventions (used in RL04). OPT and SEPT effects have been computed using IERS 05C04 polar motion time series described in section 2.1.

[19] Adding the OPT significantly influences SLR ΔC_{21} and ΔS_{21} estimates. These show seasonal variability modulated by the Chandler period. SLR ΔC_{21} and ΔS_{21} are also sensitive to the SEPT model difference, the effect is less than omitting the OPT in the original SLR processing. SLR ΔC_{21} and ΔS_{21} time series show seasonal features during the first 3 years (2002–2005) which appear to differ from those over (2005–2007). However, after including the OPT and using the newer SEPT model, revised SLR esti-

mates ("SLR-PT" in Figure 1) have more uniform seasonal variability over the entire 5 year period, and agreement with other estimates is greatly improved (see section 3).

3. Comparisons of SH Variations

[20] Figures 2a, 2b, and 2c shows monthly time series of ΔC_{21}, ΔS_{21}, and ΔC_{20} from GRACE (labeled in the figures as GRC), EOP, climate models (labeled AOW), and SLR-PT (SLR estimates after OPT and SEPT corrections). All time series have had mean values and linear trends removed. All show clear seasonal variability, especially ΔS_{21} and ΔC_{20}. GRC, EOP, AOW, and SLR-PT estimates of ΔC_{21} and ΔS_{21}, agree with each other well. All four estimates of ΔC_{20} also agree with each other, though EOP shows more interannual variability. This may be residual variations remaining after low cut filtering of the LOD series.

[21] Amplitudes and phases of annual and semiannual variations are estimated from each series using unweighted

Table 1. Amplitude and Phase of Annual and Semiannual ΔC_{21}, ΔS_{21}, and ΔC_{20} Changes Estimated From GRACE (GRC) RL04 Solutions, Earth Rotation (EOP), Geophysical Modes (AOW), and SLR. SLR-OPT Represents SLR Estimates With Ocean Pole Tide (OPT) Correction, and SLR-PT Represents SLR Estimates With Both OPT and Solid Earth Pole Tide (SEPT) Corrections[a]

	Annual		Semiannual	
Gravity Change	Amplitude, $\times 10^{-10}$	Phase, deg	Amplitude, $\times 10^{-10}$	Phase, deg
ΔC_{21} (GRC)	0.24	149	0.13	150
ΔC_{21} (EOP)	0.22	154	0.08	161
ΔC_{21} (AOW)	0.22	116	0.07	181
ΔC_{21} (SLR)	0.25	51	0.11	170
ΔC_{21} (SLR-OPT)	0.15	106	0.11	162
ΔC_{21} (SLR-PT)	0.19	139	0.11	168
ΔC_{21} (GRC-RL01)	0.86	40	0.11	117
ΔS_{21} (GRC)	0.69	109	0.19	222
ΔS_{21} (EOP)	0.69	115	0.23	238
ΔS_{21} (AOW)	0.82	104	0.17	231
ΔS_{21} (SLR)	0.35	115	0.05	185
ΔS_{21} (SLR-OPT)	0.51	113	0.05	173
ΔS_{21} (SLR-PT)	0.61	113	0.04	164
ΔS_{21} (GRC-RL01)	0.24	91	0.45	212
ΔC_{20} (GRC)	1.43	52	0.21	170
ΔC_{20} (EOP)	1.37	68	0.91	56
ΔC_{20} (AOW)	1.37	55	0.05	175
ΔC_{20} (SLR)	1.38	49	0.24	163
ΔC_{20} (SLR-Cox)	1.29	28	0.14	171
ΔC_{20} (GRC-RL01)	1.52	62	0.44	80

[a]The SEPT correction is the difference between the earlier RL01 SEPT model and the IERS2003 SEPT model used in RL04 data. The phase is defined as ϕ in $\sin(2\pi(t - t_0) + \phi)$, where t_0 refers to h_0 on 1 January. SLR ΔC_{20} from *Cox and Chao* [2002] is denoted as "SLR-Cox". Similar estimates from *Chen et al.* [2004] from GRACE RL01 (April 2002 to March 2004) are also given.

least squares, with results in Table 1. Estimates are given for the original SLR series, series with an ocean pole tide corrections (SLR-OPT), and with both OPT and SEPT corrections (SLR-PT). Table 1 also gives earlier GRACE estimates from *Chen et al.* [2004] for the period April 2002 to March 2004, (GRC-RL01), and SLR estimate of ΔC_{20} from *Cox and Chao* [2002] (SLR-Cox). Annual components of ΔC_{21}, ΔS_{21}, and ΔC_{20} are also presented as phasor plots (Figure 3).

[22] Annual variations of ΔC_{21}, ΔS_{21}, and ΔC_{20}, from GRC, EOP, AOW, and SLR-PT (for ΔC_{21}, ΔS_{21}), and SLR (for ΔC_{20}) agree very well in both amplitude and phase. As noted earlier, SLR ΔC_{21} and ΔS_{21} estimates without pole tide corrections show poorer agreement in both amplitude (ΔS_{21}) and phase (ΔC_{21}). Agreement in semiannual variations is also good, especially for ΔC_{21} and ΔS_{21}, considering that their amplitudes are relatively small. GRC and SLR semiannual ΔC_{20} estimates also agree well. In general, at seasonal periods, EOP ΔC_{21} and ΔS_{21} show the best agreement with GRC, while SLR ΔC_{20} agrees best with GRC. EOP ΔC_{20} show a strong semiannual signal (with a magnitude of 0.91×10^{-10}), consistent with earlier studies [*Chen and Wilson*, 2003; *Chen et al.*, 2004]. This is likely due to errors in atmospheric wind fields that must be subtracted to estimate ΔC_{20} from LOD. GRACE RL04 solutions significantly improve agreement with other ΔC_{21} and ΔS_{21} estimates, relative to earlier results from RL01 (see Table 1). The improvement is due to the OPT and revised SEPT model in RL04 [*Chen et al.*, 2004].

[23] Figure 4 shows intraseasonal variations of ΔC_{21}, ΔS_{21}, and ΔC_{20} from GRC, EOP, AOW, and SLR. These time series are derived by removing annual and semiannual variations in Figure 2, using coefficients in Table 1, and then removing long period variations with low cut filter removing variations longer than 1 year. There is good correlation among the 4 independent estimates of ΔC_{21}, ΔS_{21}, and ΔC_{20}. Correlation coefficients at zero lag be-
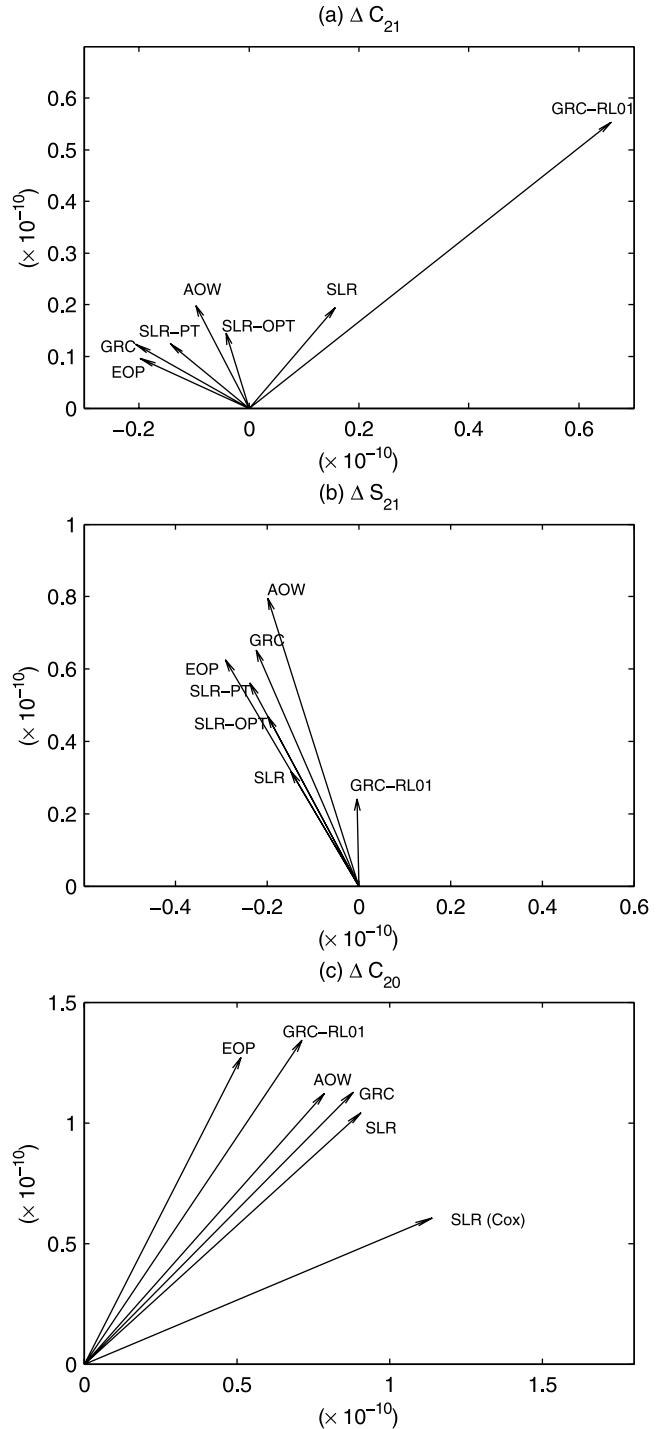
Figure 3. (a, b, and c) Phasor plots of annual ΔC_{21}, ΔS_{21}, and ΔC_{20} variations as listed in Table 1.
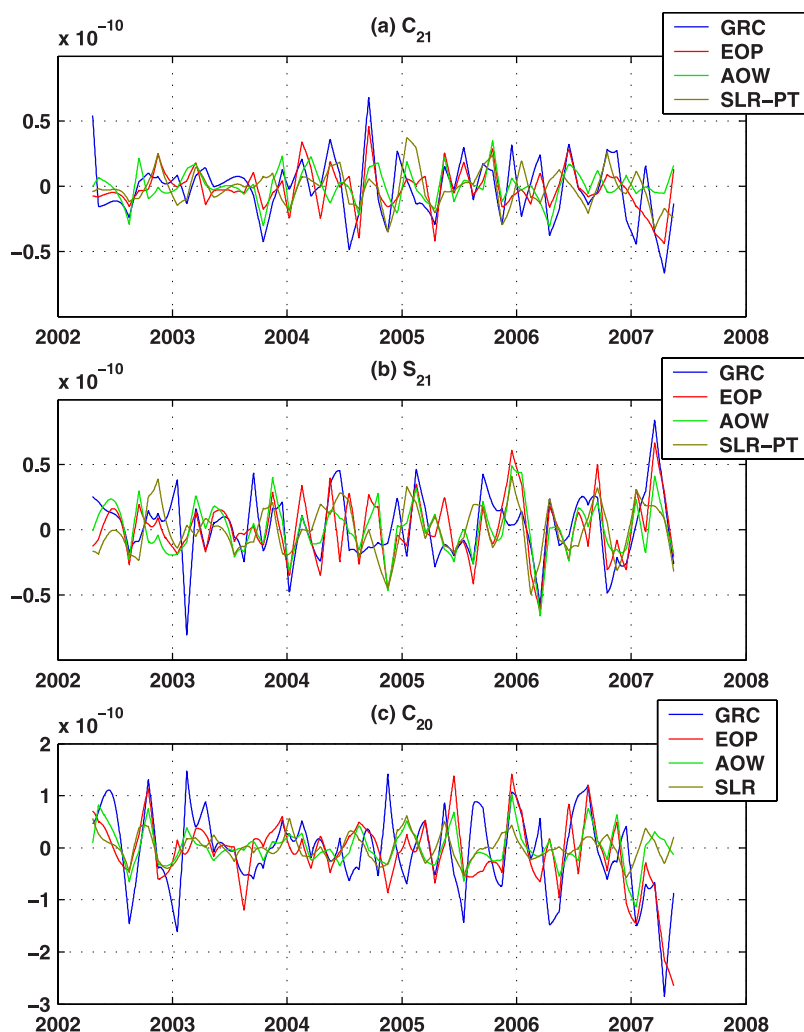
Figure 4. (a, b, and c) Intraseasonal ΔC_{21}, ΔS_{21}, and ΔC_{20} variations from GRACE (blue curves and squares), Earth rotation EOP (red curves and circles), and AOW models (green curves and triangles), and SLR (dark yellow curves and stars). All time series are averaged and resampled to match GRACE sample times. Annual and semiannual signals and variations at periods longer than 1 year are removed from all time series.

tween each pair (e.g., GRC versus EOP, denoted as GRC/EOP) were computed after interpolating each series to daily sampling, with results given in Table 2.

[24] For most time series pairs, correlation coefficients are well above the 99% significance level, about 0.32. For example, the correlation coefficients between GRC and EOP estimates of ΔC_{21}, ΔS_{21}, and ΔC_{20} are 0.66, 0.56, and 0.56, respectively. For ΔC_{21}, GRC and EOP show the best correlation (0.66), while for ΔS_{21}, the best correlation is between EOP and AOW, with a value of 0.81. Although AOW/SLR-PT shows maximum correlation for ΔC_{20} (0.75), GRC and EOP show excellent agreement with each other over the last 1.5 years of the time series, and also for ΔS_{21} (Figures 4c and 4b). Both GRC and EOP ΔC_{20} both show evidence of a similar linear drift at the end of the time series (Figures 2c and 4c), possibly due to interannual variability.

[25] Errors in the diurnal-semidiurnal ocean tide model used in GRACE data processing may contaminate GRACE time series, appearing as aliases at certain periods. For

example, it is known that errors in the S_2 tide have an alias period of 161 d [Han et al., 2005], and will contaminate time series of ΔC_{20} [Seo et al., 2008]. The RL04 tide model (FES2004) [Lyard et al., 2006] should improve the situation, but we find that ΔC_{20} is still affected by the 161-day alias, but ΔC_{21} and ΔS_{21} time series appear not to be. A

Table 2. Correlation Coefficients at Zero Lag of Intraseasonal ΔC_{21}, ΔS_{21}, and ΔC_{20} Time Series, Among Estimates From GRACE (GRC), Earth Rotation (EOP), Geophysical Models (AOW), and SLR-PT (SLR With Pole Tide Corrections)[a]

| Correlation Pair	$\Delta C21$	$\Delta S21$	$\Delta C20$
GRC/EOP	0.66	0.56	0.56
GRC/AOW	0.35	0.53	0.40
GRC/SLR-PT	0.39	0.40	0.29
EOP/AOW	0.51	0.81	0.58
EOP/SLR-PT	0.55	0.56	0.50
AOW/SLR-PT	0.33	0.52	0.75

[a]The 99% significance level is about 0.32.

power spectrum of GRC ΔC_{20} (Figure 4) shows a strong peak near a period of 161 d, in addition to an annual peak. A least squares fit 161-day sinusoid has a magnitude of about 1.12×10^{-10} and phase of ~254 degree, making this alias term nearly as large as the annual (Table 1). In addition, the GRC ΔC_{20} spectrum shows fairly large variations near a period of ~3 years in the power spectrum, possibly indicating other alias contamination (see Figure 5).

[26] With four more-or-less independent estimates of the same quantities, it is possible to compute estimates of RMS noise levels in each time series. If each series is a sum of true signal plus noise, for example [$\Delta C_{21}^{GRC} = \Delta C_{21}^{true} +$ Noise_C_{21}^{GRC}] then the difference between any two ΔC_{21} series should have a variance equal to the sum of noise variances in each, provided that the noise in different estimates is independent. We can formulate a set of 6 linear equations by taking the difference between each pair of series (in Figures 2 and 4). Prior to the calculation, variations at periods exceeding 2 years are removed with a low-cut filter, and the 161-day alias is removed from GRACE time series. The left hand side of the set of equations is the sum of noise variances to be determined, and the right hand side is the variance of the difference series.

$$\text{var}\left(Noise\_C_{21}^{GRC}\right) + \text{var}\left(Noise\_C_{21}^{EOP}\right) = \text{var}\left(\Delta C_{21}^{GRC} - \Delta C_{21}^{EOP}\right)$$

$$\text{var}\left(Noise\_C_{21}^{GRC}\right) + \text{var}\left(Noise\_C_{21}^{AOW}\right) = \text{var}\left(\Delta C_{21}^{GRC} - \Delta C_{21}^{AOW}\right)$$

$$\cdots$$

$$\text{var}\left(Noise\_C_{21}^{AOW}\right) + \text{var}\left(Noise\_C_{21}^{SLR}\right) = \text{var}\left(\Delta C_{21}^{AOW} - \Delta C_{21}^{SLR}\right)$$

$$(2)$$

[27] The least squares solution provides an estimate of noise variance for each SH time series, and their square
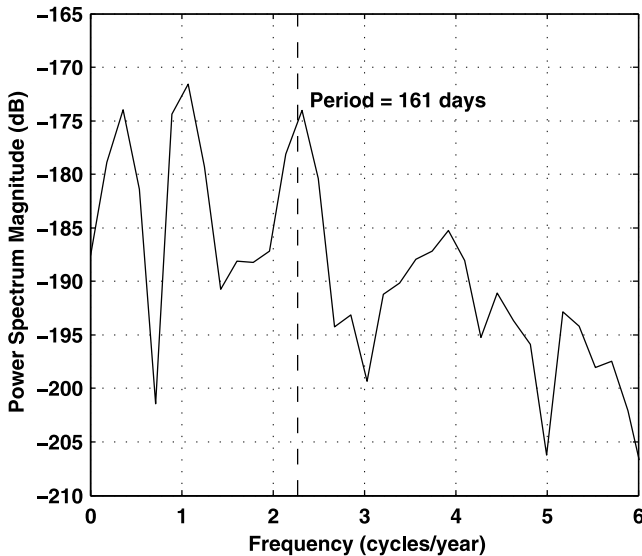
Figure 5. Power spectrum of GRACE ΔC_{20} estimates. The 58 time series values (with a few missing points) are interpolated to a uniform daily time series to compute the spectrum. The red dashed line marks the S2 tide alias period of 161 d.

Table 3. RMS Noise Level Estimates of ΔC_{21}, ΔS_{21}, and ΔC_{20}, Computed From Least Squares Fit to Variances of the Difference of Each Time Series Pair Listed in Table 2[a]

Sources	$\Delta C21$ ($\times 10^{-10}$)	$\Delta S21$ ($\times 10^{-10}$)	$\Delta C20$ ($\times 10^{-10}$)
GRC	0.22	0.28	1.37
GRC (intra)	0.21	0.23	0.70
EOP	0.13	0.15	1.01
EOP (intra)	0.09	0.14	0.51
AOW	0.17	0.17	0.33
AOW (intra)	0.14	0.10	0.22
SLR-PT	0.21	0.34	0.44
SLR-PT (intra)	0.15	0.21	0.38
GRC (for)	0.02	0.02	0.12
SLR (cal)	0.67	0.67	0.31

[a]A low cut filter has removed variations from each series at period greater than 2 years. Separate estimates denoted by "intra" are for intraseasonal time series (shown in Figure 3) and are similar to estimates made from time series that include the seasonal terms. The 161-d S_2 alias was removed from GRACE time series. GRC formal error (denoted as "for") and SLR calibration error (denoted as "cal") are listed for comparison.

roots (rms values) are given in Table 3. This calculation provides an estimate of RMS noise levels for GRC and SLR-PT (or SLR for ΔC_{20}) as an alternative to their reported formal errors. For EOP and AOW no separate estimates of noise levels are available. The RMS error estimates in Table 3 represent both observational error, and cumulative effects of various data processing steps needed to produce GRACE time series. The GRACE estimate also includes effects that cause the value to differ from a true monthly average, which is actually computed in the case of EOP and AOW. GRC formal errors (denoted as "for") and SLR calibration errors (denoted as "cal") are listed in Table 3 for comparison. GRC formal errors are much smaller than estimates derived by this method. Separate estimates denoted by "intra" are for intraseasonal time series (shown in Figure 4). For SLR, there is no reason to expect errors for ΔC_{21} and ΔS_{21} to differ, and values in Table 3 are nearly the same. For EOP, there is no reason to expect errors to be different in ΔC_{21} and ΔS_{21}, so these could be combined into a single value. For AOW, there is no reason to expect errors in any of the three components to differ. All depend on large scale averages of ocean, atmosphere and hydrologic fields, so the three could be combined as well. Table 3 shows that noise estimates for GRC, EOP, and SLR ΔC_{20} time series are all much larger than for ΔC_{21} and ΔS_{21}. GRACE ΔC_{20} has the largest estimated noise value, consistent with the discussion elsewhere.

4. Conclusions

[28] At seasonal timescales, the four separate estimates of variations in SH coefficients agree remarkably well in both amplitude and phase. For seasonal ΔC_{21} and ΔS_{21} variations, EOP estimates show the best agreement with GRC results, while SLR agrees best with GRC in ΔC_{20}. At intraseasonal timescales, the 4 independent estimates also agree very well with each other, as indicated by large correlation coefficients. GRACE RL04 solutions show improved agreement with others relative to RL01, especially for ΔC_{21} and ΔS_{21}. SLR estimates of ΔC_{21} and

ΔS_{21} are significantly altered by the OPT correction and revised SEPT model. After OPT and SEPT corrections, SLR ΔC_{21} and ΔS_{21} series agree well with the others.

5. Discussion

[29] Estimates of variations in gravity field coefficients from EOP are sensitive to errors in numerical model wind fields. This is especially true for ΔC_{20} because winds cause over 90% of LOD variations at timescales of a few years and less. Therefore excellent agreement of EOP estimates of annual variations in ΔC_{21}, ΔS_{21}, and ΔC_{20} with others (GRC, AOW, SLR) indicates that wind field variations at annual timescales are fairly well represented in the NCEP model. Agreement at the semiannual period is poorer, suggesting that wind field variations are relatively less well determined. The strong semiannual component in EOP ΔC_{20} is not a feature of the other estimates. Winds from pressure levels above 10 millibars are not included in the NCEP reanalysis model. Zonal winds at this level and above may be significant contributors to LOD [e.g., *Rosen and Salstein*, 1985; *Gross et al.*, 2004b; *Chen*, 2005], suggesting that their inclusion may improve EOP ΔC_{20} estimates.

[30] This study confirms the importance of using proper OPT and SEPT models in geodetic satellite analysis, especially in estimation of ΔC_{21} and ΔS_{21}. OPT effects on ΔC_{21} and ΔS_{21} can be comparable to nontidal influences.

[31] Independent estimates of ΔC_{21}, ΔS_{21}, and ΔC_{20} from EOP, AOW, and SLR are useful to validate GRACE measurements at SH degree 2, where GRACE errors are likely to be relatively large. In addition, intercomparison of ΔC_{21}, ΔS_{21}, and ΔC_{20} variations are useful in identifying and quantifying errors associated with each technique. As examples, this study confirms the importance of OPT and SEPT for SLR and suggests the importance of upper atmospheric winds for EOP ΔC_{20} estimates. Because they represent global averages, accurately determined degree-2 SH changes should continue to be important in monitoring large-scale mass variations in the atmosphere, ocean, hydrosphere, and cryosphere at a variety of timescales.

Acronyms

CSR	Center for Space Research
DLR	German Aerospace Center
ECCO	Estimating the Circulation and Climate of the Ocean
EOP	Earth Orientation Parameters
GLDAS	global land data assimilation system
GPS	Global Positioning System
GRACE	Gravity Recovery and Climate Experiment
LOD	length-of-day
NASA	National Aeronautics and Space Administration
NCEP	National Centers for Environmental Prediction
OPT	ocean pole tide
PGR	postglacial rebound
PT	pole tide
PL01	release 1
RL04	release 4
SCEQ	self-consistent equilibrium
SEPT	Solid Earth Pole Tide
SH	spherical harmonic
SLR	satellite laser ranging

References

Aoyama, Y., and I. Naito (2000), Wind contribution to the Earth's angular momentum budgets in seasonal variations, *J. Geophys. Res.*, *105*(D10), 12,417–12,431.

Bettadpur, S. (2003), CSR level-2 processing standards document for product release 01, GRACE 327-742, revision 1.0, the GRACE project, Center for Space Research, Univ. of Texas, Austin.

Bettadpur, S. (2007a), Level-2 gravity field product user handbook, GRACE 327-734, revision 2.3, the GRACE project, Center for Space Research, Univ. of Texas, Austin.

Bettadpur, S. (2007b), CSR level-2 processing standards document for product release 04, GRACE 327-742, revision 3.1, the GRACE project, Center for Space Research, Univ. of Texas, Austin.

Chao, B. F., and R. J. Eanes (1995), Global gravitational changes due to atmospheric mass redistribution as observed by the LAGEOS nodal residual, *Geophys. J. Int.*, *122*, 755–764.

Chen, J. L. (2005), Global mass balance and the length-of-day variation, *J. Geophys. Res.*, *110*, B08404, 10.1029/2004JB003474.

Chen, J. L., and C. R. Wilson (2003), Low degree gravitational changes from Earth rotation and geophysical models, *Geophys. Res. Lett.*, *30*(24), 2257, doi:10.1029/2003GL018688.

Chen, J. L., C. R. Wilson, R. J. Eanes, and B. D. Tapley (2000), A new assessment of long wavelength gravitational variations, *J. Geophys. Res.*, *105*(B7), 16,271–16,278.

Chen, J. L., C. R. Wilson, B. D. Tapley, and J. Ries (2004), Low degree gravitational changes from GRACE: Validation and interpretation, *Geophys. Res. Lett.*, *31*, L22607, doi:10.1029/2004GL021670.

Chen, J. L., C. R. Wilson, B. D. Tapley, and S. Grand (2007), GRACE detects coseismic and postseismic deformation from the Sumatra-Andaman earthquake, *Geophys. Res. Lett.*, *34*, L13302, doi:10.1029/2007GL030356.

Cheng, M. K., and J. Ries (2007), Monthly estimates of C20 from 5 SLR satellites, GRACE technical note #05, the GRACE project, Center for Space Research, Univ. of Texas, Austin.

Cheng, M., and B. D. Tapley (2004), Variations in the Earth's oblateness during the past 28 years, *J. Geophys. Res.*, *109*, B09402, doi:10.1029/2004JB003028.

Cheng, M. K., C. K. Shum, and B. Tapley (1997), Determination of long-term changes in Earth's gravity field from satellite ranging observations, *J. Geophys. Res.*, *102*(B10), 22,377–22,390.

Cox, C. M., and B. F. Chao (2002), Detection of a large-scale mass redistribution in the terrestrial system since 1998, *Science*, *297*, 831–833.

Desai, S. (2002), Observing the pole tide with satellite altimetry, *J. Geophys. Res.*, *107*(C11), 3186, doi:10.1029/2001JC001224.

Devoti, R., V. Luceri, C. Sciarretta, G. Bianco, G. Di Donato, L. L. A. Vermeersen, and R. Sabadini (2001), The SLR secular gravity variations and their impact on the inference of mantle rheology and lithospheric thickness, *Geophys. Res. Lett.*, *28*(5), 855–858.

Dickey, J. O., S. L. Marcus, Oliver de Viron, and I. Fukumori (2002), Recent Earth oblateness variations: Unraveling climate and postglacial rebound effects, *Science*, *298*, 1975–1977.

Dong, D., R. S. Gross, and J. O. Dickey (1996), Seasonal variations of the Earth's gravitational field: An analysis of atmospheric pressure, ocean tidal, and surface water excitation, *Geophys. Res. Lett.*, *23*(7), 725–728.

Eubanks, T. M. (1993), Variations in the orientation of the Earth, in *Contributions of Space Geodesy to Geodynamic: Earth Dynamics*, Geodyn. Ser., vol. 24, edited by D. Smith and D. Turcotte, pp. 1–54, AGU, Washington, D. C.

Fukumori, I., T. Lee, D. Menemenlis, L.-L. Fu, B. Cheng, B. Tang, Z. Xing, and R. Giering (2000), A dual assimilation system for satellite altimetry, Joint TOPEX/POSEIDON and Jason-1 Science Working Team Meeting, Miami Beach, Fla., 15–17 November.

Gross, R. S., G. Blewitt, P. J. Clarke, and D. Lavallée (2004a), Degree-2 harmonics of the Earth's mass load estimated from GPS and Earth rotation data, *Geophys. Res. Lett.*, *31*, L07601, doi:10.1029/2004GL019589.

Gross, R. S., I. Fukumori, D. Menemenlis, and P. Gegout (2004b), Atmospheric and oceanic excitation of length-of-day variations during 1980–2000, *J. Geophys. Res.*, *109*, B01406, doi:10.1029/2003JB002432.

Han, S.-C., C. K. Shum, and K. Matsumoto (2005), GRACE observations of M2 and S2 ocean tides underneath the Filchner-Ronne and Larsen ice

shelves, Antarctica, *Geophys. Res. Lett.*, *32*, L20311, doi:10.1029/2005GL024296.

Johnson, T. J., C. R. Wilson, and B. F. Chao (1999), Oceanic angular momentum variability estimated from the Parallel Ocean Climate Model, 1988–1998, *J. Geophys. Res.*, *104*(B11), 25,183–25,196.

Kalnay, E. M., et al. (1996), The NCEP/NCAR 40-year reanalysis project, *Bull. Am. Meteorol. Soc.*, *77*, 437–471.

Lemoine, F., et al. (1998), *The Development of the Joint NASA GSFC and the NIMA Geopotential Model EGM96*, NASA/TP-1998-206861, Goddard Space Flight Center, Greenbelt, Maryland.

Lyard, F., F. Lefevre, T. Letellier, and O. Francis (2006), Modelling the global ocean tides: Insights from FES2004, *Ocean Dyn.*, *56*, 394–415.

McCarthy, D. D., and G. Petit (Eds.) (2003), IERS conventions, IERS tech. note 32, Int. Earth Rotation and Ref. Syst. Serv., Paris.

Mitrovica, J. X., and W. R. Peltier (1993), Present-day secular variations in the zonal harmonics of Earth's geopotential, *J. Geophys. Res.*, *98*(B3), 44,509–44,526.

Rodell, M., et al. (2004), The global land data assimilation system, *Bull. Am. Meteorol. Soc.*, *85*(3), 381–394.

Rosen, R. D., and D. A. Salstein (1985), Contribution of stratospheric winds to annual and semi-annual fluctuations in atmospheric angular momentum and the length of day, *J. Geophys. Res.*, *90*(D5), 8033–8041.

Rubincam, D. P. (1984), Postglacial rebound observed by Lageos and the effective viscosity of the lower mantle, *J. Geophys. Res.*, *89*(B2), 1077–1087.

Seo, K-.W., C. R. Wilson, J. L. Chen, and D. E. Waliser (2008), GRACE's spatial aliasing error, *Geophys. J. Int.*, *172*(1), 41–48.

Tapley, B. D., S. Bettadpur, M. M. Watkins, and C. Reigber (2004), The gravity recovery and climate experiment: Mission overview and early results, *Geophys. Res. Lett.*, *31*, L09607, 10.1029/2004GL019920.

Tapley, B., et al. (2005), GGM02 an improved Earth gravity field model from GRACE, *J. Geod.*, *79*, 467–478, doi:10.1007/s00190-005-0480-z.

Wahr, J. M. (1982), The effects of the atmosphere and oceans on the earth's wobble. Part I: Theory, *Geophys. J.*, *70*, 349–372.

Wahr, J. (1985), Deformation induced by polar motion, *J. Geophys. Res.*, *90*(B11), 9363–9368.

Wahr, J., M. Molenaar, and F. Bryan (1998), Time-variability of the Earth's gravity field: Hydrological and oceanic effects and their possible detection using GRACE, *J. Geophys. Res.*, *103*(B12), 30,205–30,229.

Wahr, J., S. Swenson, V. Zlotnicki, and I. Velicogna (2004), Time-variable gravity from GRACE: First results, *Geophys. Res. Lett.*, *31*, L11501, doi:10.1029/2004GL019779.

Yoder, C. F., J. G. Williams, J. O. Dickey, B. E. Schutz, R. J. Eanes, and B. D. Tapley (1983), Secular variation of Earth's gravitational harmonic J coefficient from Lageos and non-tidal acceleration of Earth rotation, *Nature*, *303*, 757–762.

Zhou, Y. H., D. Salstein, and J. L. Chen (2006), Revised atmospheric excitation function series related to Earth's variable rotation under consideration of surface topography, *J. Geophys. Res.*, *111*, D12108, doi:10.1029/2005JD006608.

―――――――――――

J. L. Chen and C. R. Wilson, Center for Space Research, University of Texas, NULL, 3925 West Braker Lane, Suite 200, Austin, TX 78712-5321, USA. (chen@csr.utexas.edu)